

Fragile, Robust, and Antifragile: A Perspective from Parameter Responses in Reinforcement Learning Under Stress

Zain ul Abdeen

*Bradley Department of Electrical and Computer Engineering
Virginia Tech.
Blacksburg, VA 24060, USA*

ZABDEEN@VT.EDU

Ming Jin

*Bradley Department of Electrical and Computer Engineering
Virginia Tech.
Blacksburg, VA 24060, USA*

JINMING@VT.EDU

Abstract

This paper explores Reinforcement learning (RL) policy robustness by systematically analyzing network parameters under internal and external stresses. Inspired by synaptic plasticity in neuroscience, synaptic filtering introduces internal stress by selectively perturbing parameters, while adversarial attacks apply external stress through modified agent observations. This dual approach enables the classification of parameters as *fragile*, *robust*, or *antifragile*, based on their influence on policy performance in clean and adversarial settings. Parameter scores are defined to quantify these characteristics, and the framework is validated on PPO-trained agents in Mujoco continuous control environments. The results highlight the presence of antifragile parameters that enhance policy performance under stress, demonstrating the potential of targeted filtering techniques to improve RL policy adaptability. These insights provide a foundation for future advancements in the design of robust and antifragile RL systems.

Keywords: Reinforcement Learning, Antifragility, Synaptic Filtering, Policy Robustness.

1. Introduction

RL Scalable Approach for Safe and Robust Learning via Lipschitz-Constrained Networks has demonstrated success in solving complex decision-making tasks across diverse domains, including robotics [Tang \(2024\)](#), game playing [Yuan \(2024\)](#), autonomous systems [Zhang \(2022\)](#); [ul Abdeen \(2024\)](#), and the alignment of large language models [Ziegler \(2019\)](#). Despite these achievements, RL agents exhibit vulnerabilities to various perturbations, highlighting the need for a deeper understanding of their capacity to adapt and generalize in dynamic and adversarial environments [Li \(2022\)](#); [Nagy \(2023\)](#).

This study proposes a stress-testing framework to systematically evaluate RL agents under two forms of stress: (i) *internal stress*, involving parameter perturbations through synaptic filtering of the RL policy network, inspired by synaptic stress applications in neuroscience [Oken \(2015\)](#); [Citri \(2008\)](#), and (ii) *external stress*, induced by adversarial perturbations to the agent observations [Kurakin \(2018\)](#). Through this dual analysis, we characterize policy network parameters as **fragile**, **robust**, or **antifragile**. Building on Taleb’s concept of antifragility [Taleb \(2014\)](#), we define antifragility in RL as the ability of a policy to not only withstand stress but to improve performance under such stresses.

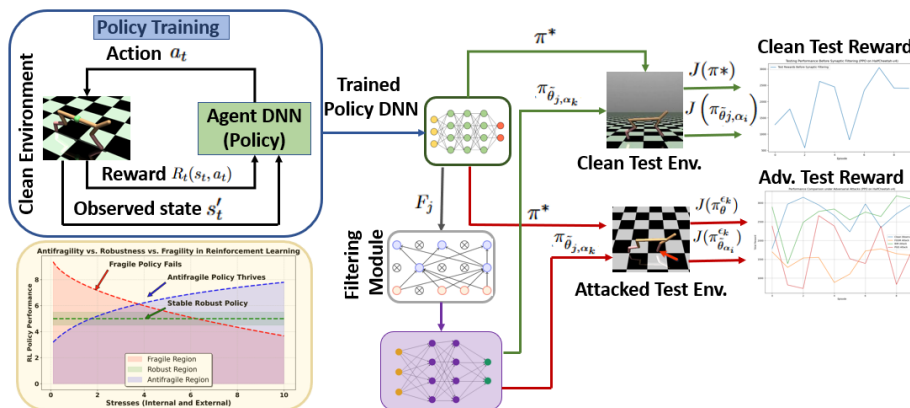


Figure 1: Framework for training and evaluating robust and antifragile policies in RL.

To achieve this framework, we apply signal processing technique to induce internal stress by perturbing network parameters, thereby simulating parameter sensitivity, and employ adversarial attacks to impose external stress on agents observation. This dual approach distinguishes our method from traditional random filtering methods [Srivastava \(2014\)](#); [Yu \(2018\)](#). Systematically varying the magnitude of these stressors, we assess their impact on agent performance. Parameters critical to performance degradation are labeled as *fragile*, while those unaffected by stress are identified as *robust*. Parameters that contribute to improved performance under stress are classified as *antifragile*, providing insights into the resilience and adaptability of RL agents. Figure 1 illustrates this categorization, showing how RL agent performance varies under different levels of stress.

We validate our approach using agents trained with the Proximal Policy Optimization (PPO) algorithm [Schulman \(2017\)](#) in continuous control environments from the OpenAI Gym benchmark suite [Brockman \(2016\)](#), which provide diverse challenges for evaluating RL policy robustness. Our results show that introducing controlled stressors reveals parameter vulnerabilities and identifies antifragile characteristics, offering a pathway for designing more resilient and adaptive RL systems.

The key contributions of this work are: (1) introducing the concept of antifragility to RL, demonstrating that controlled stressors can enhance performance and extend robustness; (2) proposing a framework to evaluate RL agents under internal stress (via synaptic filtering) and external stress (via adversarial attacks); and (3) classifying policy parameters as fragile, robust, or antifragile, providing insights into parameter sensitivity and resilience.

2. Related work

Antifragility has gained traction in fields like robotics [Axenie \(2023\)](#), economics [Manso \(2019\)](#) and medicine [Axenie \(2022\)](#). In machine learning and control theory, it often addresses resilience to black swan events [Jin \(2024\)](#); [Sun \(2024\)](#). Chandresh et. al. [Pravin \(2024\)](#), introduced antifragility in deep learning, as scenarios where stresses lead to performance improvements. Internal stress involves perturbing policy network parameters, inspired by pruning techniques [Ramanujan \(2020\)](#); [Molchanov \(2019\)](#), which typically aim to reduce network size while maintaining performance. However, under certain conditions, filtering parameters can enhance performance, whilst being subjected to internal and external stress, in the form of synaptic filters [Mariet \(2015\)](#) and adversarial

attacks [Dabholkar \(2024\)](#). Unlike these methods, our approach extends this by employing synaptic filtering to evaluate RL policies in clean and adversarial environments, characterizing parameters as fragile, robust, or antifragile. External stress focuses on adversarial attacks like FGSM [Huang \(2017\)](#) and PGD [Zhang \(2020\)](#), which exploit RL policies’ sensitivity to adversarial examples in real-world applications. Ilyas et al. [Ilyas \(2019\)](#) distinguished between robust and non-robust features, offering insights into parameter sensitivity under stress. Given the sequential nature of RL decision-making [Qiaoben \(2024\)](#), analyzing adversarial attacks is critical. We use FGSM to systematically assess the impact of adversarial perturbations, providing a framework to characterize policy parameters under stress.

3. Preliminaries

3.1. Markov decision process (MDP)

RL is a computational approach where an agent learns to make decisions by interacting with an environment to maximize cumulative rewards. Formally, RL is modeled as a finite MDP, represented by the tuple $\mathcal{M} = (\mathcal{S}, \mathcal{A}, T, P, R)$, where \mathcal{S} and \mathcal{A} are the state and action spaces, and T is the horizon length. The environment dynamics defined by $P = \{P_t(s'_t|s_t, a_t)\}_{t=1}^T$, gives the probability of transition from state $s_t \in \mathcal{S}$ to $s'_t \in \mathcal{S}$ given action $a_t \in \mathcal{A}$ at time step t . $R = \{R_t(s_t, a_t)\}_{t=1}^T$ denotes the immediate reward function. The agent follows a policy $\pi : \mathcal{S} \times \mathcal{A} \rightarrow [0, 1]$, where $\pi(a|s)$ is the probability of selecting action a in state s . The goal is to find an optimal policy π^* that maximizes the expected cumulative reward $J(\pi)$ from any initial state s_0 :

$$\pi_{a_t|s_t}^* = \arg \max_{\pi} J(\pi) = \arg \max_{\pi} \mathbb{E}_{a_t \sim \pi} \left[\sum_{t=0}^T R_t(s_t, a_t) \right] \quad (1)$$

We employ policy-based RL algorithm, which directly optimize in the policy space to achieve the maximization in (1), and policy is instantiated using a deep neural network, i.e., $\pi_{\theta}(a_t|s_t)$, where θ represents the parameters (weights and biases) of the policy network. Following a given policy $\pi_{\theta}(a_t|s_t)$, the RL controller performance can be written as $J(\theta) = \mathbb{E}_{a_t \sim \pi_{\theta}} \left[\sum_{t=0}^T R_t(s_t, a_t) \right]$. Therefore, objective becomes optimizing policy parameters, i.e., $\theta^* = \arg \max_{\theta} J(\theta)$. To this end, we use PPO algorithm, use gradient ascent for policy update: $\theta_{t+1} = \theta_t + \eta \hat{\nabla}_{\theta} J(\theta)$, where $\hat{\nabla}_{\theta} J(\theta)$ is the policy gradient estimated from collected experience, and η is the learning rate.

3.2. External Stress

External stress in RL refers to factors that negatively impact an agent performance by disrupting its interaction with the environment, such as changes in observations, actions, or environment dynamics [Sun \(2020\)](#). In our investigation, FGSM is utilized, a computationally efficient technique for generating adversarial examples through single-step perturbations. FGSM creates these perturbations by modifying the input state based on the gradient of the loss function. For an observation state s_t , an adversarial perturbation δ_{ϵ} of magnitude ϵ is calculated as $\delta_{\epsilon} = \epsilon \cdot \text{sign}(\nabla_{s_t} J(\theta, s_t))$. The perturbation observation is then $s_t^{\epsilon} = s_t + \delta_{\epsilon}$. The loss function used for generating the adversarial perturbation is defined as $J(\theta, s_t) = -\log \pi_{\theta}(a_t|s_t)$. Maximizing this loss reduces the agent confidence in its chosen action, potentially leading to suboptimal or incorrect decisions. External stress is applied with various magnitudes $\epsilon = \epsilon_0, \epsilon_1, \dots, \epsilon_M$, ranging from a minimum (ϵ_0) to a

maximum perturbation magnitude ϵ_M with a step size $\Delta\epsilon$. This results in a set of perturbed observations $\mathcal{S}_\epsilon = [s_t^{\epsilon_0}, s_t^{\epsilon_1}, \dots, s_t^{\epsilon_M}]$ for the agent. The set of policy networks under external stress defined as:

$$\Pi^\epsilon = [\pi_\theta(a_t|s_t^{\epsilon_0}), \pi_\theta(a_t|s_t^{\epsilon_1}), \dots, \pi_\theta(a_t|s_t^{\epsilon_M})]. \quad (2)$$

Analyzing the performance of the agent under varying levels of external stress assesses policy robustness to external stress. The cumulative rewards obtained under different magnitudes as:

$$\mathcal{J}^\epsilon = [J(\pi_\theta^{\epsilon_0}), J(\pi_\theta^{\epsilon_1}), \dots, J(\pi_\theta^{\epsilon_M})] \quad (3)$$

Examining how \mathcal{J}^ϵ varies with increasing ϵ quantifies performance degradation due to adversarial attacks. This approach identifies the specific perturbation magnitudes required to significantly degrade performance or cause agent failure.

4. Methodology for Policy Characterization

In this section, we detail the methodology employed to characterize the policy parameters as fragile, robust, or antifragile under internal and external stress. Our approach involves applying synaptic filtering as internal stress to the policy network of an RL agent. This section first explain how we apply the internal stress and then introduce parameter scores that characterize the parameters.

4.1. Internal Stress

Internal stress involves perturbing the parameters of policy network $\pi_\theta(\cdot)$ to evaluate their impact on performance. We implement this through **synaptic filtering**, which systematically modifies or removes parameters based on their magnitudes. Formally, synaptic filtering in RL is defined as: ‘‘Given a policy network $\pi_\theta(\cdot)$ with parameters $\theta \in \mathbf{R}^n$. Synaptic filtering applies a mask $m_\alpha \in \{0, 1\}^n$ determined by a filtering function $F_\alpha(\cdot)$. The filtered parameters $\tilde{\theta}$ are obtained as:

$$\tilde{\theta} = F_\alpha(\pi_\theta) = m_\alpha \odot \theta, \quad (4)$$

where \odot denotes the element-wise Hadamard product’’. The mask m_α is determined by the filtering method and threshold α , where $\alpha = \{\alpha_0, \alpha_1, \dots, \alpha_N\}$ represent a normalized set of synaptic filtering thresholds spanning the entire parameter range with lower bound $\alpha_0 = \min\{|\theta|\}$, upper bound $\alpha_N = \max\{|\theta|\}$, and step size $\Delta\alpha = \frac{\alpha_N - \alpha_0}{N}$ such that $\alpha_i = \alpha_{i-1} + \Delta\alpha$. For meaningful analysis, all policy parameters satisfies ($\theta \neq 0$); otherwise, the policy network $\pi_\theta(\cdot)$ produces invalid outputs.

4.1.1. SYNAPTIC FILTERING METHODS

We investigate three types of synaptic filters: F_{HPF} , the High-pass Filter; F_{LPF} , the ideal Low-pass Filter; F_{PWF} the Pulse Wave Filter, each with distinct properties. We apply the filtering operations to the trained policy network π_θ with parameters θ and are defined as follows:

High-Pass Filter (F_{HPF}): This filter zeroes out parameters whose absolute values below threshold α_i , removing weaker synaptic connections. The filtered parameters $\tilde{\theta}_{1,\alpha_i}$ are obtained by:

$$\tilde{\theta}_{1,\alpha_i} = F_{HPF}(\theta, \alpha_i) = \begin{cases} 0, & \text{if } |\theta| \leq \alpha_i, \\ \theta, & \text{otherwise.} \end{cases} \quad (5)$$

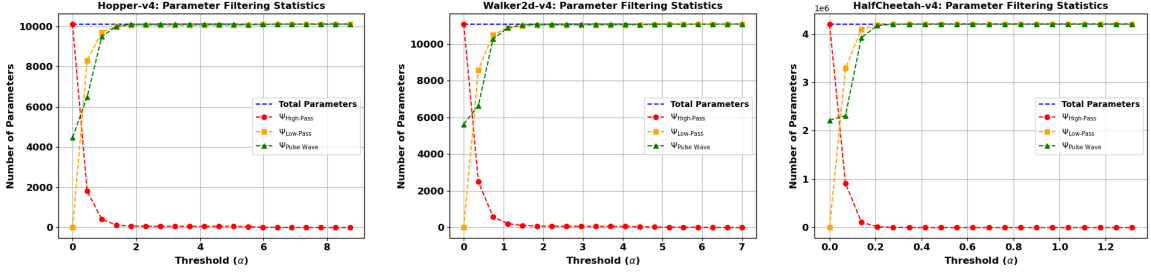


Figure 2: Global parameter filtering statics for mujoco environment

where $\alpha_i \in \alpha$, and we increment α_i by $\Delta\alpha$ at each step from $\alpha_0 = \min(|\theta|)$ to $\alpha_k = \max(|\theta|)$.

Low-Pass Filter (F_{LPF}): For a given threshold α_i , the filtered parameters $\tilde{\theta}_{2,\alpha_i}$ are defined as:

$$\tilde{\theta}_{2,\alpha_i} = F_{LPF}(\theta, \alpha_i) = \begin{cases} 0, & \text{if } |\theta| \geq \alpha_i, \\ \theta, & \text{otherwise.} \end{cases} \quad (6)$$

Here, α_i decreases from $\alpha_k = \max(|\theta|)$ to $\alpha_0 = \min(|\theta|)$, decrementing by $\Delta\alpha$ at each step. Low-Pass filter tests if smaller weights contribute to robustness or antifragility.

Pulse Wave Filter (F_{PWF}): For a given threshold α_i , the filtered parameters $\tilde{\theta}_{3,\alpha_i}$ are given by:

$$\tilde{\theta}_{3,\alpha_i} = F_{PWF}(\theta, \alpha_i) = \begin{cases} 0, & \text{if } \alpha_i - \frac{\Delta\alpha}{2} < |\theta| \leq \alpha_i + \frac{\Delta\alpha}{2}, \\ \theta, & \text{otherwise.} \end{cases} \quad (7)$$

This filter zeroes out parameters within a small window around the threshold α_i , effectively creating a moving pulse that assesses the impact of mid-range parameters on policy performance.

For each filter F_j , we define the network *compactness*: $\Psi_{j,\alpha_i} = 1 - \frac{\psi_{j,\alpha_i}}{\psi}$ as the portion of parameter retained after filtering, where ψ is the total number of parameters and ψ_{j,α_i} is the number of parameters filtered out by filter. The figure (2) illustrates the distribution of parameter magnitudes, showing that the High-Pass Filter removes most parameters at low thresholds, indicating a concentration of small-magnitude parameters. By systematically varying α_i , these filters generate three sets of perturbed parameters:

$$\tilde{\Theta}_1 = \{\tilde{\theta}_{1,\alpha_i} \text{ for } \alpha_i \in \alpha\}, \quad \tilde{\Theta}_2 = \{\tilde{\theta}_{2,\alpha_i} \text{ for } \alpha_i \in \alpha\}, \quad \tilde{\Theta}_3 = \{\tilde{\theta}_{3,\alpha_i} \text{ for } \alpha_i \in \alpha\}. \quad (8)$$

Correspondingly, we obtain three sets of perturbed policy networks:

$$\Pi_1 = \{\pi_{\tilde{\theta}_{1,\alpha_i}}(\cdot) \mid \alpha_i \in \alpha\}, \quad \Pi_2 = \{\pi_{\tilde{\theta}_{2,\alpha_i}}(\cdot) \mid \alpha_i \in \alpha\}, \quad \Pi_3 = \{\pi_{\tilde{\theta}_{3,\alpha_i}}(\cdot) \mid \alpha_i \in \alpha\}. \quad (9)$$

By applying these filters to the policy parameters, we assess the agent ability to make decisions and achieve rewards when its internal parameters are perturbed. This analysis helps us understand the sensitivity of the policy performance to changes in different regions of the parameter space. For each filter F_j (where $j \in \{\text{HPF}, \text{LPF}, \text{PWF}\}$), we measure the cumulative rewards:

$$\mathcal{J}_{j,\alpha} = [J(\pi_{\tilde{\theta}_{j,\alpha_0}}), J(\pi_{\tilde{\theta}_{j,\alpha_1}}), \dots, J(\pi_{\tilde{\theta}_{j,\alpha_k}})], \quad (10)$$

where, $J(\pi_{\tilde{\theta}_{j,\alpha_i}})$ represents the cumulative reward achieved by perturbed policy $\pi_{\tilde{\theta}_{j,\alpha_i}}$. Comparing these results to unperturbed policy performance $J(\pi_\theta)$ quantifies the impact of internal stress.

4.2. Parameter Characterization

In this subsection we define the three characterizations of policy parameters: *fragility*, *robustness* and *antifragility*. In order to define these characterizations, we define parameter score as metric which measure the performance of perturbed and unperturbed policy networks.

4.2.1. PARAMETER SCORE

The *parameter score* quantifies the effect of stress on policy performance. It is defined as the difference in performance between the stressed policy and the baseline policy

$$S \approx \int_{\sigma_{min}}^{\sigma_{max}} J_{stressed}(\sigma) - J_{baseline}(\sigma) d\sigma, \quad (11)$$

where, $J_{stressed}$ is the expected cumulative reward under stress, either $J(\pi_{\tilde{\theta}_{\alpha_i}})$ for internal stress or $J(\pi_{\theta}^{\epsilon_j})$ for external stress. $J_{baseline} = J(\pi_{\theta})$ is the expected cumulative reward of the baseline, unperturbed policy. The parameter score S thus captures the net effect of stress on cumulative reward received by the agent.

Parameter Score for Clean Environment: This metric measures the impact of synaptic filtering under clean environment at different thresholds α_i on the agent performance. It is computed as:

$$S_{\alpha_i} = J(\pi_{\tilde{\theta}_{\alpha_i}}) - J(\pi_{\theta}). \quad (12)$$

Assessing the parameter score in a clean environment allows us to assess the intrinsic sensitivity of the policy network to internal perturbations. By systematically filtering parameters and observing the resultant change in performance, we can identify which parameters are critical for maintaining performance (*robust*), which negatively impact performance when perturbed (*fragile*), and which enhance performance upon modification (*antifragile*). This metric provides a foundational understanding of parameter importance and resilience within the network’s architecture.

Parameter Score Under Adversarial Environment: When external stress is introduced via adversarial attacks with perturbation magnitude ϵ_k , the parameter score is calculated as:

$$S^{\epsilon_k} = J(\pi_{\tilde{\theta}_{\alpha_i}}^{\epsilon_k}) - J(\pi_{\theta}^{\epsilon_k}). \quad (13)$$

Evaluating the parameter score under adversarial environments allows us to understand how synaptic filtering influences the resilience of policy network to external perturbations. This analysis reveals whether certain parameters not only maintain performance under normal conditions but also enhance or diminish robustness against adversarial attacks.

Combined Difference of Parameter Scores: To evaluate the interplay between internal and external stresses, we compute the combined parameter score:

$$\Delta S_{\alpha_i}^{\epsilon_k} = J(\pi_{\tilde{\theta}_{\alpha_i}}^{\epsilon_k}) - J(\pi_{\tilde{\theta}_{\alpha_i}}). \quad (14)$$

The combined parameter score captures how adversarial attacks affect a synaptically filtered network compared to its clean, filtered counterpart. This metric highlights the differential impact of adversarial stress on the network after internal perturbations, providing a nuanced understanding of parameter resilience and adaptability. It helps identify parameters that not only sustain performance under internal stress but also enhance or diminish robustness against external threats.

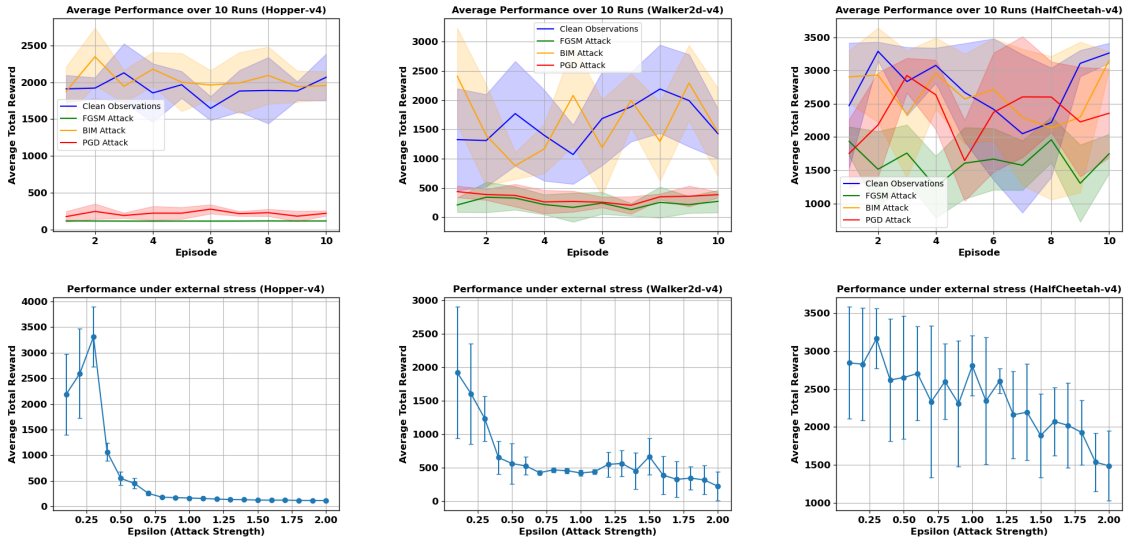


Figure 3: Impact of FGSM, BIM, and PGD Attacks on Policy Performance on Mujoco Environments.

5. Experimental Framework and Antifragility Analysis of RL Policies

5.1. Experiment Setup

We conducted experiments on three continuous control environments from the Gymnasium library: Walker2D-v4, Hopper-v4, and HalfCheetah-v4. These environments were selected for their high-dimensional state spaces and challenging control tasks, making them suitable for testing policy robustness and antifragility. The RL policies were trained using the PPO algorithm, implemented with the Stable-Baselines3 framework Raffin (2021). Both the policy and value networks used a multilayer perceptron (MLP) architecture with three hidden layers containing 512, 256, and 128 neurons, activated by ReLU function. Training process was conducted with a learning rate of 1×10^{-4} and a batch size of 128. Performance was evaluated using cumulative rewards over multiple episodes. The trained policies were subjected to stress conditions, including **synaptic filtering** and **adversarial perturbations**, to analyze their robustness, fragility, and antifragility.

5.2. Results and Discussions

Under clean conditions, trained policies achieved stable cumulative rewards across all environments, see Figure 3. Walker2D policies exhibited the highest baseline rewards 2000, indicating effective learning and stability. Hopper policies also performed well but showed slightly higher variability in rewards, suggesting increased sensitivity to parameter perturbations. HalfCheetah policies achieved moderate rewards 2500 with some variability, likely due to its high-dimensional state-action space. These baseline results establish a reference for evaluating the effects of internal and external stresses.

5.2.1. PERFORMANCE UNDER ADVERSARIAL STRESS

To evaluate policy robustness, we subjected the trained policies to three gradient-based adversarial attacks—FGSM, BIM, and PGD—with varying perturbation magnitudes ϵ . As illustrated in Figure 3, FGSM consistently inflicted the most immediate damage by saturating the ϵ -ball in a single gradient step and causing large reward drops in both `Walker2D` and `Hopper`, where returns fell near zero for $\epsilon \geq 0.5$, thereby exposing a critical *vulnerability in the parameter space* and highlighting the *fragility* of these policies to rapid, gradient-driven perturbations. By contrast, the iterative attacks (BIM and PGD) introduced smaller cumulative shifts—due partly to re-sampling and repeated clipping—and thus were *less impactful* overall, though they still revealed *robustness limitations* at higher ϵ values. In `Walker2D`, the policy showed a steady decline in returns with increasing ϵ , stabilizing at 500 for $\epsilon \geq 1.0$. `Hopper` demonstrated even greater *sensitivity*, with rewards dropping to near zero at moderate attack strengths ($\epsilon \geq 0.5$), highlighting a critical vulnerability in the parameter space. In contrast, `HalfCheetah` consistently exhibited more *resilience*, retaining moderate rewards (around 1500) even under large adversarial shifts $\epsilon = 2.0$, suggesting the presence of *robust* or potentially *antifragile* components in its policy network that adapt to stress and preserve functionality.

5.2.2. PERFORMANCE UNDER INTERNAL STRESS

To evaluate the impact of synaptic filtering methods—HPF, LPF and PWF—were applied to selectively modify policy network parameters. Parameter scores in clean (S_{α_i}) and adversarial (S^{ϵ_k}) conditions were computed to quantify performance changes at various thresholds α_i .

Parameter Scores for Clean Environments: The left column of Figure 4 shows parameter scores (S_{α_i}) under clean environment. Across all environments, high-pass filter consistently yields large negative scores at all thresholds α . This indicates the presence of **fragile** parameters, as the removal of these parameters leads to significant degradation in the policy performance. Conversely, the low-pass filter shows positive parameter scores at certain thresholds (e.g., $\alpha = 2-4$ in `Hopper` and `Walker2D`), indicate **antifragile** behavior, where removing high-magnitude parameters improves performance. This suggests that high-frequency components may hinder optimal execution. The pulse wave filter exhibits mixed behavior. In `HalfCheetah`, low thresholds ($0.3 \leq \alpha \leq 1.1$) yields positive scores, highlighting antifragility, while higher thresholds result in negative scores, revealing fragility. This indicates that the pulse wave filter’s impact is dependent on the filtering threshold. These results emphasize the utility of low-pass filtering in identifying antifragile parameters.

Parameter Scores for Adversarial Environments: The middle column of Figure 4, examine the parameters scores S^{ϵ_k} under adversarial perturbations $\epsilon = 2.0$, providing insights into how synaptic filtering interacts with external stress. The high-pass filter continues to show highly negative scores indicating that fragile parameters identified in clean environments remain fragile under adversarial stress. The degradation is further exacerbated by external perturbations. The low-pass filter maintains its antifragility, although the magnitude of positive scores decreases slightly compared to the clean environment. This indicates that parameters identified as **antifragile** under clean conditions are also **robust** to adversarial attacks, as evident in `Hopper` and `Walker2D`. Increased fragility is observed under adversarial conditions, particularly in `HalfCheetah`, where most thresholds yield negative scores. This underscores the limited robustness of pulse wave fil-

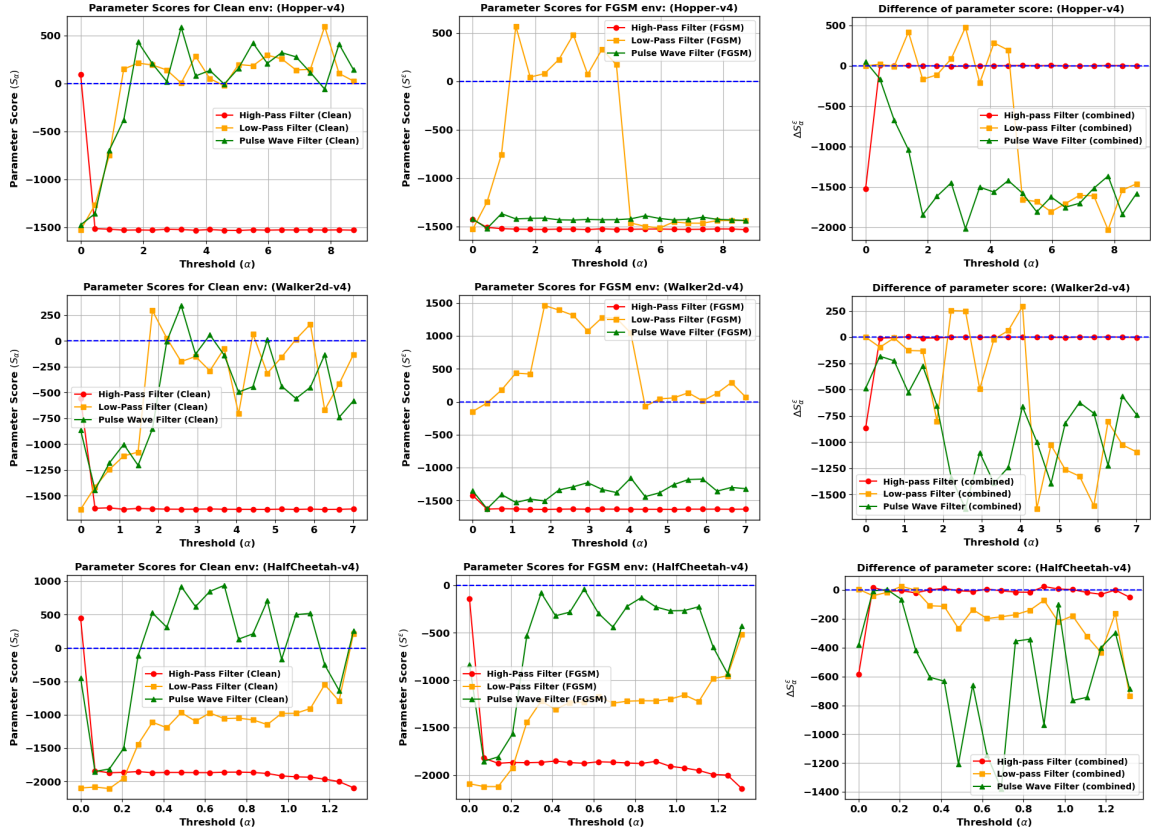


Figure 4: The left column shows parameter scores (S_{α_i}) for clean environments. The middle column shows parameter scores (S^{ϵ_k}) under FGSM adversarial perturbations with $\epsilon = 2.0$, while the right column depicts the difference in parameter scores ($\Delta S_{\alpha_i}^{\epsilon_k}$).

tering approach. The trends highlight the resilience of low-pass filtering under adversarial stress, maintaining antifragility in key parameter regions.

The heatmaps in Figure 5 illustrate the variation of parameter scores S^{ϵ_k} with internal stress (α) and external stress (ϵ), providing insights into parameter behavior under combined stress conditions. The high-pass filter predominantly identifies fragile parameters, as indicated by consistent performance degradation across thresholds and stress levels. The low-pass filter, in contrast, reveals regions of antifragility, particularly in *Walker2D-v4* and *Hopper-v4*, where moderate thresholds ($\alpha = 1.84 - 4.06$, $\alpha = 0.92 - 4.59$) and stress levels ($\epsilon = 0 - 5$) exhibit improved performance due to the removal of high-frequency components. These findings suggest that low-pass filtering isolates parameters critical for stability and balance in these environments. In *HalfCheetah-v4*, antifragility is observed at lower thresholds ($\alpha = 1.11 - 1.32$) and moderate stress levels ($\epsilon \leq 2.38$), though performance declines as external stress increases, indicating reduced resilience in this context. The pulse wave filter displays heterogeneous behavior, showing antifragility at low thresholds and mild stress ($\epsilon \leq 0.2$) but revealing fragility at higher stress levels, reflecting its sensitivity to stress conditions. Overall, the results highlight the potential of low-pass filtering to identify pa-

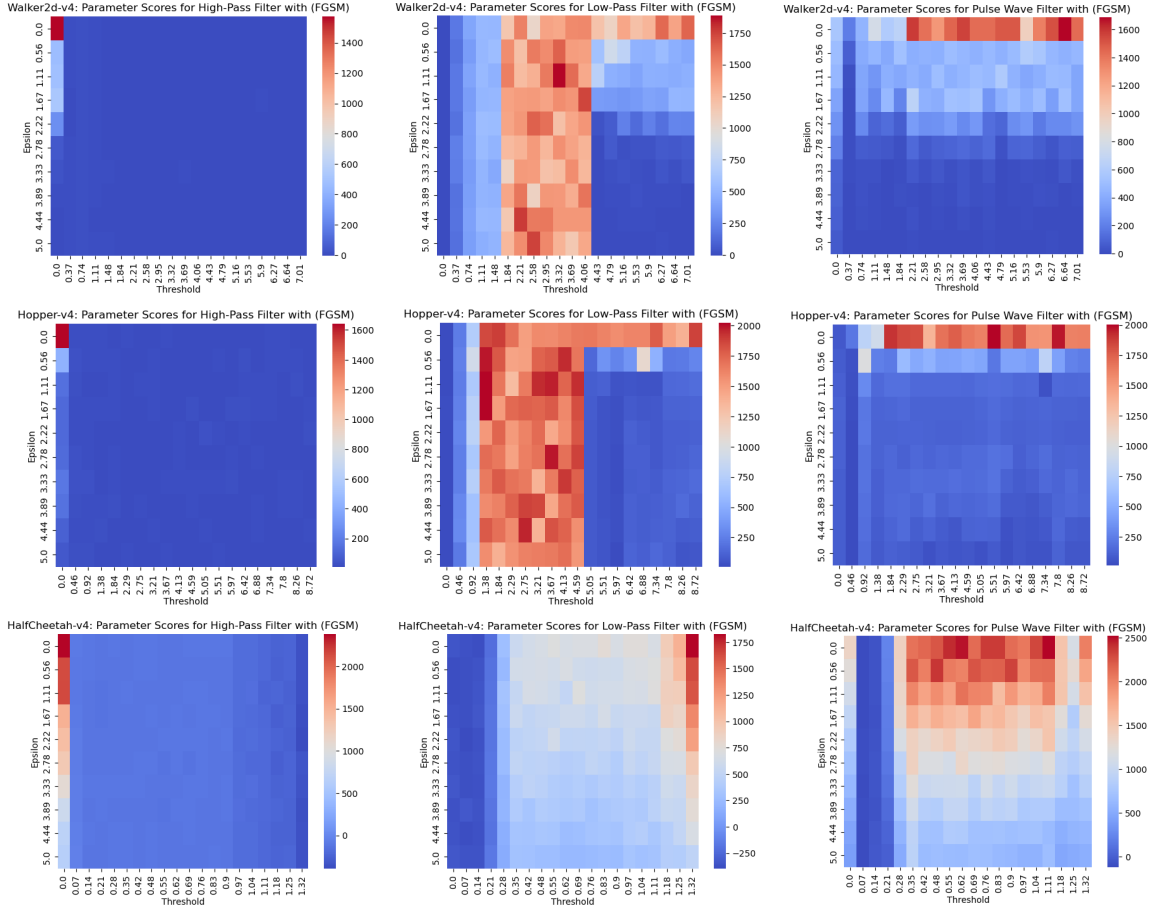


Figure 5: Heatmaps of parameter scores under FGSM adversarial attack across environments, showing synaptic filtering methods (High-Pass, Low-Pass, Pulse Wave). The x-axis represents filtering thresholds α , and the y-axis denotes stress magnitudes ϵ . Red indicates antifragility, blue indicates fragility.

rameters that contribute to policy robustness and adaptability, particularly in environments where stability plays a critical role.

Difference of Parameter Scores: The third column in Figure 4 illustrates the difference in parameter scores ($\Delta S_{\alpha_i}^{\epsilon_k}$), quantifying the impact of adversarial attacks on synaptic filtering performance. Low-pass filtering shows minimal deviation in $\Delta S_{\alpha_i}^{\epsilon_k}$, indicating robust parameter identification that performs consistently in both clean and adversarial conditions. In contrast, the pulse wave filter exhibits high variability, with sharp positive and negative deviations, highlighting its sensitivity to adversarial stress and reduced robustness compared to low-pass filtering. These findings confirm that low-pass filtering is the most effective strategy for isolating stable parameters under combined internal and external stress.

6. Conclusion and Future Directions

This study provides a detailed analysis of synaptic filtering on policy network under clean and adversarial conditions. Low-pass filtering consistently identifies robust and antifragile parameters, demonstrating its effectiveness in enhancing network resilience. High-pass filtering highlights fragile parameters that degrade performance, particularly under adversarial stress, while pulse wave filtering shows limited reliability, identifying antifragility only under specific thresholds. These findings underscore the importance of targeted filtering strategies to optimize policy performance in stress-prone environments. We are working on integrating synaptic filtering into the training process to foster the emergence of parameters that not only maintain performance under nominal conditions but also adapt and improve resilience against adversarial attacks.

References

- Cristian Axenie and Matteo Saveriano. Antifragile control systems: The case of mobile robot trajectory tracking under uncertainty and volatility. *IEEE Access*, 2023.
- Cristian Axenie, Daria Kurz, and Matteo Saveriano. Antifragile control systems: The case of an anti-symmetric network model of the tumor-immune-drug interactions. *Symmetry*, 14(10):2034, 2022.
- G. Brockman. OpenAI Gym. arXiv preprint arXiv:1606.01540, 2016.
- Ami Citri and Robert C. Malenka. Synaptic plasticity: multiple forms, functions, and mechanisms. *Neuropsychopharmacology*, 33(1):18–41, 2008.
- Ahaan Dabholkar, James Z. Hare, Mark Mittrick, John Richardson, Nicholas Waytowich, Priya Narayanan, and Saurabh Bagchi. Adversarial attacks on reinforcement learning agents for command and control. *The Journal of Defense Modeling and Simulation*, 2024.
- Sandy Huang, Nicolas Papernot, Ian Goodfellow, Yan Duan, and Pieter Abbeel. Adversarial attacks on neural network policies. arXiv preprint arXiv:1702.02284, 2017.
- Andrew Ilyas, Shibani Santurkar, Dimitris Tsipras, Logan Engstrom, Brandon Tran, and Aleksander Madry. Adversarial examples are not bugs, they are features. *NeurIPS*, 2019.
- Ming Jin. Preparing for black swans: The antifragility imperative for machine learning. arXiv preprint arXiv:2405.11397, 2024.
- Alexey Kurakin, Ian J. Goodfellow, and Samy Bengio. Adversarial examples in the physical world. In *Artificial Intelligence Safety and Security*, pages 99–112, Chapman and Hall/CRC, 2018.
- Yuxi Li. Reinforcement learning in practice: Opportunities and challenges. arXiv preprint arXiv:2202.11296, 2022.
- Gustavo Manso, Benjamin Balsmeier, and Lee Fleming. Heterogeneous innovation and the antifragile economy. Unpublished Working Paper, 2019.
- Zelda Mariet and Suvrit Sra. Diversity networks: Neural network compression using determinantal point processes. arXiv preprint arXiv:1511.05077, 2015.

- Pavlo Molchanov, Arun Mallya, Stephen Tyree, Iuri Frosio, and Jan Kautz. Importance estimation for neural network pruning. In *CVPR*, pages 11264–11272, 2019.
- Zoltan Nagy et al. Ten questions concerning reinforcement learning for building energy management. *Building and Environment*, 241:110435, 2023.
- Barry S. Oken, Irina Chamine, and Wayne Wakeland. A systems approach to stress, stressors and resilience in humans. *Behavioural Brain Research*, 282:144–154, 2015.
- Chandresh Pravin, Ivan Martino, Giuseppe Nicosia, and Varun Ojha. Fragility, robustness and antifragility in deep learning. *Artificial Intelligence*, 327:104060, 2024.
- You Qiaoben et al. Understanding adversarial attacks on observations in deep reinforcement learning. *Science China Information Sciences*, 67(5):1–15, 2024.
- Antonin Raffin et al. Stable-baselines3: Reliable reinforcement learning implementations. *Journal of Machine Learning Research*, 22(268):1–8, 2021.
- Vivek Ramanujan et al. What’s hidden in a randomly weighted neural network? In *CVPR*, pages 11893–11902, 2020.
- John Schulman et al. Proximal policy optimization algorithms. arXiv preprint arXiv:1707.06347, 2017.
- Nitish Srivastava et al. Dropout: a simple way to prevent neural networks from overfitting. *Journal of Machine Learning Research*, 15(1):1929–1958, 2014.
- Jianwen Sun et al. Stealthy and efficient adversarial attacks against deep reinforcement learning. In *AAAI*, 34:5883–5891, 2020.
- Linghang Sun et al. Antifragile perimeter control: Anticipating and gaining from disruptions with reinforcement learning. arXiv preprint arXiv:2402.12665, 2024.
- Nassim Nicholas Taleb. *Antifragile: Things That Gain from Disorder*. Random House Trade Paperbacks, 2014.
- Chen Tang et al. Deep reinforcement learning for robotics: A survey of real-world successes. arXiv preprint arXiv:2408.03539, 2024.
- Zain ul Abdeen et al. Enhancing distribution system resilience: A first-order meta-rl algorithm for critical load restoration. In *SmartGridComm*, pages 129–134, 2024.
- Ruichi Yu et al. NISP: Pruning networks using neuron importance score propagation. In *CVPR*, pages 9194–9203, 2018.
- Chengping Yuan et al. Multi-agent dual level reinforcement learning of strategy and tactics in competitive games. *Results in Control and Optimization*, 16:100471, 2024.
- Huan Zhang et al. Robust deep reinforcement learning against adversarial perturbations on state observations. *NeurIPS*, 33:21024–21037, 2020.

Zhenyi Zhang et al. Reinforcement learning behavioral control for nonlinear autonomous system. *IEEE/CAA Journal of Automatica Sinica*, 9(9):1561–1573, 2022.

Daniel M. Ziegler et al. Fine-tuning language models from human preferences. arXiv preprint arXiv:1909.08593, 2019.